Document downloaded from:

http://hdl.handle.net/10251/50904

This paper must be cited as:

Payri Marín, R.; Gimeno García, J.; Marti Aldaravi, P.; Bracho León, GC. (2013). Study of the influence of the inlet boundary conditions in a LES simulation of internal flow in a diesel injector. Mathematical and Computer Modelling. 57(7-8):1709-1715. doi:10.1016/j.mcm.2011.11.019.

The final publication is available at

http://dx.doi.org/10.1016/j.mcm.2011.11.019

Copyright Elsevier

Study of the influence of the inlet boundary conditions in a LES simulation of internal flow in a diesel injector

Raul Payri[a], Jaime Gimeno[a,*], Pedro Marti-Aldaravi[a], Gabriela Bracho[b]

[a] *CMT - Motores Térmicos, Universidad Politécnica de Valencia, Edificio 6D, 46022, Valencia, Spain*
[b] *GE Global Research Europe, Freisinger Landstrasse 50 D-85748 Garching bei Munchen, Germany*

Abstract

In this paper the study of the behavior of the fuel flow through the injector nozzle using CFD tools is presented. Large Eddy Simulation will be used to model the internal flow turbulence in a Diesel fuel injector with velocities over 500 m/s. More specifically, the influence of boundary conditions applied to the model will be studied. The article analyses the influence of the inlet boundary condition upon activation and maintenance of turbulent flow during the calculation. Carefully assessing which inlet boundary condition is more trustworthy with reality, for this the outlet velocity, pressure, turbulence and level of stabilization will be studied.

Keywords: Large Eddy Simulation, Diesel injectors, Internal flow, Inlet boundary, Turbulence.

*Corresponding author.
Email addresses: rpayri@mot.upv.es (Raul Payri), jaigigar@mot.upv.es (Jaime Gimeno), pedmar15@mot.upv.es (Pedro Marti-Aldaravi), Gabriela.Bracholeon@ge.com (Gabriela Bracho)

Preprint submitted to Mathematical and Computer Modelling 57 (2013) 1709-1715 December 3, 2013

	Nomenclature	Units
A^+	Van Driest Function Constant	-
C_s	Smagorinsky Model Constant	-
C_v	Velocity coefficient	-
l	Mixing length	m
$\dot{m}$	Mass flow flux	kg/s
$\dot{M}$	Momentum flux	N
p	Pressure	MPa
S	Rate of strain tensor	1/s
t	Time	s
u	Velocity	m/s
u_τ	Wall shear	$m^{5/2}/(kg^{1/2} \cdot s)$
y^+	Wall distance in viscous wall units	$m^{3/2}/kg^{1/2}$
Δ	Local grid scale	m
δ	Kronecker Delta (Identity tensor)	-
ρ	Fuel density	kg/m^3
τ	Stress-like tensor	m^2/s^2
ν	Fuel kinematic viscosity	m^2/s
ν_t	Turbulent viscosity	m^2/s

1. Introduction

Realistic boundary conditions are necessary in numerical simulations in order to get validated results, and much research is being done about it. In computational fluid dynamics it is widely accepted that the fluid behaviour is determined in large part by the inlet behaviour, especially in turbulent flows. For Reynolds Averaged Navier-Stokes (RANS) simulations, only mean profiles of velocity or pressure and some turbulent variables need to be defined at the inlet, but for Large-Eddy (LES) and Direct-Numerical (DNS) Simultaions the turbulent inflow conditions have to be prescribed, which is much more of an issue [1].

In DNS all scales of motion are calculated, so it is expensive for any turbulent flow. In RANS an averaging process is applied to the flow equations to divide them into a mean flow and fluctuations around that mean, called "turbulence", then, only the mean flow is calculated and the fluctuations are estimated by a model. In LES it is assumed that only large-scales of motion are affected by the geometry of the domain while the small-scales are similar or even self-similar in the bulk of the flow, then, the averaging applied to the flow equations is a spatial averaging in the form of a convolution filter, separating the flow into grid scale (GS) and sub-grid scale (SGS) components. The GS motion is explicitly simulated whilst the average effect of the SGS on GS motion is taken into account by a SGS model [2].

The power of LES for modelling real systems has been proved, concretely R. Payri et al. [3] have shown the accuracy of this code for simulating the internal flow in diesel injectors. However, no comparison of fluid behaviour in real systems with different inlet boundary conditions has been found. For example, G. R. Tabor et al. [4] made a review of synthesised and precursor simulation methods for defining the inlet, but the domain was squared channel. Thus, in the present work the main idea is to simulate the internal

flow of a diesel injector in order to check the accuracy of three different already available inlet conditions. The results are compared and validated with experimental data.

2. Methodology

2.1. Case description

As commented before, LES code is applied to an industrial process, such a modern common-rail nozzle injector in diesel engines [5, 6]. The pressure gradient in these systems is very high and the fluid experiences a restriction, which could affect in the flow in a way the boundary layer detaches and the flow along the hole becomes turbulent. The study is focused just to the liquid phase inside nozzle (no cavitation is considered) [7], and the main goal is to find the most suitable inlet boundary condition.

The nozzle geometry is the same that used in previous works [3, 8]. It corresponds to an axi-symmetric nozzle manufactured specially for research purposes. The orifice has an outlet diameter of 112 µm and 1 mm of length. The shape is convergent, thus the cavitation is "avoided" [9] and the assumption that simulation involves only incompressible liquid is validated.

The conditions are characterized by two inlet pressures, 120 MPa and 160 MPa, correspondig to medium and high diesel injection pressures and an outlet pressure of 5 MPa. Isothermal conditions are assumed and the temperature used for the simulations was 298 K. The working fluid was winter diesel fuel with a constant density of 825.28 kg/m^3 and also constant viscosity of $2.80 \cdot 10^{-3}$ kg/(m $\cdot$ s) [10].

The Reynolds number based on the theoretical Bernouilli velocity and the exit diameter is 17400 for medium injection pressure case and 20200 for high injection pressure case. Both values are high enough to expect the flow to be turbulent. Before the calculation it was unknown if the turbulence is fully developed because the hole could not be long enough.

Figure 1 shows the computational mesh used in this study. It is the same that was used in previous works [3, 8]. The size of the mesh is around 1.5 million cells.

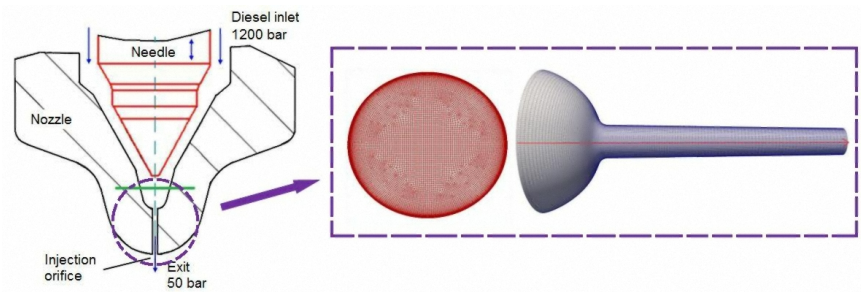

Figure 1: Nozzle geometry used for the simulations on the left. Computational domain and mesh of the simulated volume on the right.

The boundary conditions used in the simulations are described below. Inlet conditions are detailed in the next subsection.

- Walls: non-slip velocity condition.
- Outlet: uniform pressure condition was used, and zero gradient velocity setup [8].

2.2. Inlet conditions

Three different inlet conditions were tested. According to [4], the inlet boudary should:

- be stocahstically varying;
- ... on scales down to the filter scale (spatially and temporally);
- be compatible with Navier-Stoke equations;
- "look" like turbulence;
- allow the easy specification of turbulent properties;
- and be easy to implement and to adjust to new inlet conditions.

However, the chosen inlet conditions do not meet all of these requirements. They are:

- Constant pressure: uniform pressure condition and zero gradient velocity setup. When the pressure is known at the inlet, the velocity is evaluated from the flux, normal to the patch.
- Turbulent inlet: similar to the previous condition, but a random Gaussian noise is added over pressure variable (with an amplitude of 5% [11, 12]), thus generating oscillations in the flow. It "looks" like turbulence, but does not reproduce the coherent structures and the oscillations could be quickly damped because of that.
- Mapped inlet (or direct mapped): internal mapping condition in which a precursor domain is integrated in the main domain. This method uses a scaling mapping of the pressure field at a section in the interior of the domain to reproduce the turbulent behaviour at the inlet.

Constant pressure inlet is the most common and the simplest condition in computational fluid dynamics [13], and that is why it was taken for this study. Turbulent inlet is the easiest way to introduce oscillations in the flow field, although they do not have the structure of the turbulence. And direct mapped condition meets all the requirements listed above, but as every precursor method is more expensive in computational cost than the other two because the domain is larger.

Comparing direct mapped with other precursor methods, like prepared library calculated by a cyclic domain, is faster. The main drawback of it, despite the computational cost, is that some perturbations could travel upstream and reach the mapped plane, thus they will be copied to the inlet. This feedback could lead into instabilities in the calculus, but the solution is just setting the entry section far enough upstream from any instability of the main domain. That distance is, at least, 4 times longer than the size of the entry of the main domain. In this study an extra domain 5 times longer in legth and with the same diameter was added to the main domain, as shown in Figure 2. The resulting mesh has more than 3.8 millions cells, more than twice the main domain.

Figure 2: Sketch of the domain showing the extra volume, the main volume and the mapped section.

2.3. Cases

Two different cases were studied, high and medium injection pressures. And each case was solved three times: first with a constant pressure inlet, second with a turbulent inlet, and third with a direct mapped condition. So a total of 6 calculations were performed. Details of these cases can be found in Table 1.

Case name	**Mesh size**	**Inlet pressure**	**Inlet boundary**
1200_simple	1455300	120 MPa	Constant
1200_turbulent	1455300	120 MPa	Turbulent
1200_mapped	3880756	120 MPa	Mapped
1600_simple	1455300	160 MPa	Constant
1600_turbulent	1455300	160 MPa	Turbulent
1600_mapped	3880756	160 MPa	Mapped

Table 1: Case description.

3. Computational calculation

3.1. Mathematical formulation

The numerical simulation of the Navier-Stokes equations has been carried out using LES. The basics of the LES technique has been reported in several previous studies [14, 15]. The governing equations for flow field are the well known continuity and momentum equations. The filtered version of these equations are Equations 1 and 2, where the symbol "$\bar{x}$" means filtered variable.

$$\nabla \cdot \bar{u} = 0 \tag{1}$$

$$\frac{\partial \bar{u}}{\partial t} + \nabla \cdot \bar{u}\bar{u} = -\frac{1}{\rho}\nabla \bar{p} + \nu \nabla^2 \bar{u} - \nabla \tau \tag{2}$$

Equations 1 and 2 govern the large (energy-carrying) scales of motion and the SGS stress tensor τ is the modelled term which also provides the communication between the resolved scales and the dissipation scales [15].

In general, the purpose of the sub-grid scale is to remove energy from the resolved scales, imitating the forward energy cascade mechanism to the sub-grid scales. Usually, and in this work, it is assumed that the anisotropic part of τ is related to the resolved strain rate field through a scalar eddy viscosity ν_t [14]:

$$\tau - \frac{\delta}{3} tr(\tau) = -2\nu_t \bar{S} \tag{3}$$

where δ is the Kronecker delta (or Identity tensor) and S is the second invariant of the large scale strain tensor:

$$\bar{S}_{ij} = (\partial \bar{u}_i / \partial \bar{x}_j + \partial \bar{u}_j / \partial \bar{x}_i)/2 \tag{4}$$

The model used for estimate the turbulent eddy viscosity ν_t is the Smagorinsky Model, widely used in internal flow calculations, in where it is supposed that ν_t is proportional to the SGS characteristic length Δ and to a characteristic SGS velocity:

$$\nu_t = (C_s \Delta)^2 \left(2\|\bar{S}\|^2\right)^{1/2} \tag{5}$$

where C_s is a theoretical value of 0.1-0.2 and $\Delta = (\Delta x \Delta y \Delta z)^{1/3}$ is measured of the local grid length scale, which varies spatially.

The presence of a solid wall modifies the turbulence dynamics, inducing inhomogeneity and anisotropy in the flow. In this region, fluid properties become dependent on the distance to the wall. So, it has been shown that the turbulent eddy viscosity must be modified by using a wall damping that switches off the eddy viscosity in the near-wall region [14]. The wall damping function used in this work is the also widely used van Driest damping, where the mixing length $l = C_s \Delta$ is modified by:

$$l = C_s \Delta \left[1 - \exp\left(-\frac{y^+}{A^+}\right)\right]^{1/2} \tag{6}$$

where y^+ is the distance from the wall in viscous wall units $y^+ = y u_\tau / \nu$, the friction velocity is $u_\tau = \sqrt{\tau_{wall}/\rho}$, τ_{wall} is the wall shear and A^+ is a dimensionless constant with an empirical value of 26.

Numerical schemes used for solving the equations are quite important in LES due to they define the accuracy, stability and speed of the simulation. In this case, as in previous works [3], a backward implicit second order scheme has been used for time derivatives, Gauss linear schemes for gradients, divergences and Laplace operators, and linear for interpolation between cell values.

3.2. Procedure

The governing equations presented in the previous subsection are solved using the finite volume CFD code OpenFOAM 1.5 [12], which employs temporal and spatial discretisation schemes that are bounded and preserve the proper physical limits on the fluid-dynamics variables. The solution procedure employs the *Oodles* solver, which is a generic single-phase incompressible LES solver.

Computer cluster called "Tirant" was used for the calculus. "Tirant" is composed of 256 blade JS20 IBM computers, each one with 2 processors PowerPC 970+ and 4GB of RAM memory. Four of them (8 nucleis) were used for more than 3 months to perform all the calculus presented in this work.

4. Results and discussion

In the following sections the results of the simulations are presented. The first part of the analysis is made comparing the three calculus of each case. Then, the simulations are validated with experimental data obtained by [9].

4.1. Time evolution

First, a comparison of the instantaneous velocity trend is made. Figure 3 shows the sections and points for it. In each section, three points have been taken: one at half channel and two at the ends, far enough from the boundary to avoid wall effects. Only the stabilized time will be shown, the previous trend is always the same, the velocity grows from zero to the mean value, with a peak before it stabilizes, as shown in Figure 4.

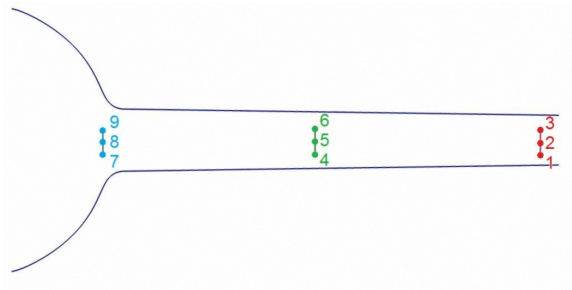

Figure 3: Sections and points chosen for plotting the instantaneous velocity. Entry: points 7, 8 and 9. Middle: points 4, 5 and 6. Exit: points 1, 2 and 3.

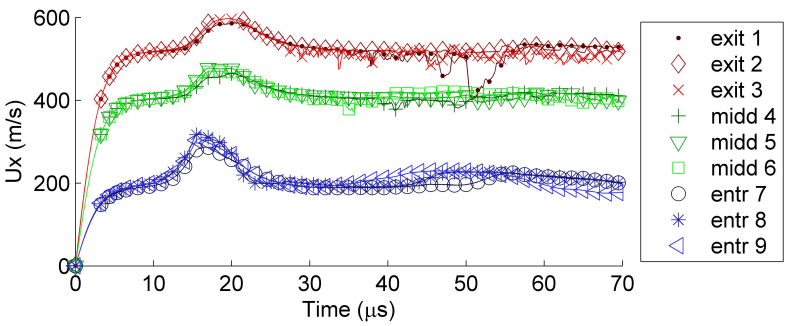

Figure 4: Velocity time evolution in three different sections for the 120 MPa injection pressure case with a constant pressure boundary inlet.

The stabilization time is defined as the simulated time at which the oscillations have appeared and the flow is stabilized in time. Table 2 summarizes this time for every simulation. It can be seen, in both cases, that the turbulent inlet aids the oscillations to appear. Direct mapped inlet stabilizes the flow even in less time, but this does not mean

mapped inlet is the fastest option, the domain is more than double so the computing time will be larger (more than double). A strange value is obtained for 160 MPa injection pressure case and turbulent inlet condition. A value around 47 ms was expected. This low value could be due to the way of defining the stabilization time, as the oscillations are higher for high injection pressure, the range for the "stabilized averaged" velocity is larger and it is reached sooner.

Case name	**Stabilization time** [ms]
1200_simple	60.6395
1200_turbulent	43.969
1200_mapped	23.865
1600_simple	64.9329
1600_turbulent	24.978
1600_mapped	27.565

Table 2: Stabilization time for every simulation made.

Figure 5 shows the velocity time evolution for 120 MPa injection pressure case. Figure 5a shows the expected result, the turbulence is generated at the restriction (entrance of the hole) and developed along the hole. So, there are no oscillations at the entry section, some at the middle and more at the exit. The behaviour with the turbulent inlet is the same, shown in Figure 5b, but some oscillations can be observed at the entry. This is because of the artifical oscillations that the boundary is imposing close to the entry section. Nevertheless, no oscillations at all can be seen for the mapped inlet simulation. No turbulence is generated with this boundary. The same fluid behaviour is observed for the high injection pressure case.

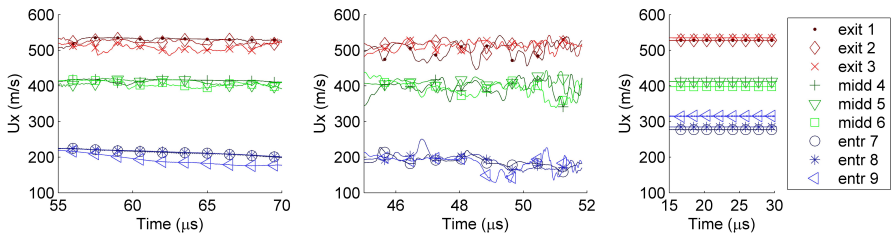

(a) Constant pressure (b) Turbulent (c) Mapped

Figure 5: Velocity time evolution for stabilized flow in three different sections for the 120 MPa injection pressure case.

4.2. Turbulent viscosity contours

The differences in the velocity field are already studied in the previous section, and almost no differences can be seen in the pressure field, though turbulent viscosity contours reveal interesting information.

Figure 6 shows them for the 120 MPa injection pressure case. With the constant pressure boundary we can see how turbulence is generated at the restriction and how it develops along the hole. With the turbulent inlet much more turbulence is observed at the inlet, obviously because the boundary is generating oscillations in the flow. However with the direct mapped almost no turbulence is obtained, just some at the restriction and at the boundary layer close to the wall. Looking at that, the authors think that some oscillations in the flow after the restriction could apear by simulating more time. Again, the discussion is the same for the high injection pressure case.

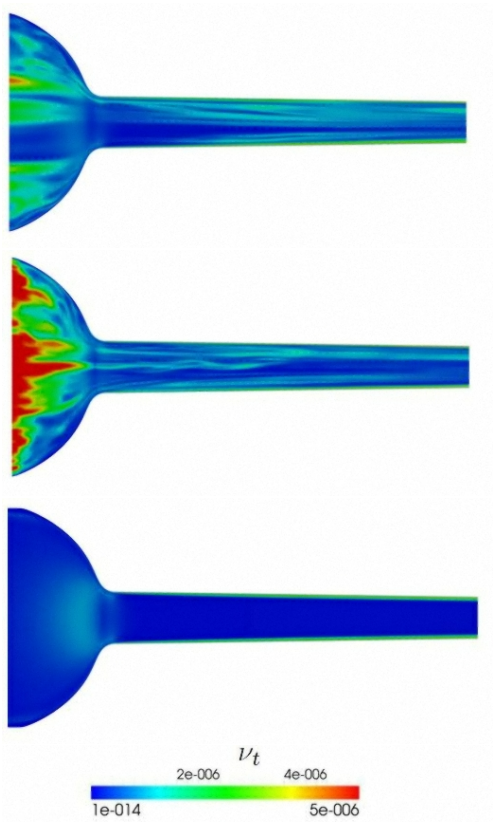

Figure 6: Turbulent viscosity ν_t contours for 120 MPa injection pressure. From the top to the bottom: constant pressure inlet, turbulent inlet and mapped inlet.

4.3. Validation using experimental results

The simulation results are compared against equivalent experimental data performed in [9]. In particular, in [9] special devices were used to obtain some dimensionless coefficients, all described in such work.

The parameter used for comparison purposes is C_v, as defined by [16] and shown in Equation 7. This coefficient measures how much the exit flow deviates from the ideal

Bernoulli flow at the exit. It was chosen because it is dimensionless and it does not depend on the outlet diameter, therefore possible errors due to differences between real diameter and simulated one are avoided [16]. The comparison between the experimental and simulated values is summarized in Table 3. As can be seen, constant pressure inlet estimates the experimental value very well meanwhile turbulent boundary overestimates it and direct mapped underestimates slightly. This is probably due to the oscillations. With this result any inlet condition can be dismissed, the three of them are in a range narrow enough to say that they are right, especially considering the error in the experimental measurement.

$$C_v = \frac{u_{eff}}{u_{Berno}} = \frac{u_{eff}}{\sqrt{2\Delta p/\rho}}; \quad u_{eff} = \frac{\dot{M}}{\dot{m}} \tag{7}$$

Case name	C_v [-]	$C_v\|_{exp}$ [-]	**Deviation** [%]
1200_simple	0.902	0.907	−0.569
1200_turbulent	0.912	0.907	0.619
1200_mapped	0.888	0.907	−2.034
1600_simple	0.908	0.909	−0.166
1600_turbulent	0.964	0.909	6.025
1600_mapped	0.909	0.909	−0.002

Table 3: Simulated and experimental velocity coefficient values and deviation between them.

5. Conclusions

A study of the influence in LES of three common inlet boundary conditions on a real system has been done. Calculus has been validated and the fluid behaviour has been analized obtaining the following conclusions.

There are big differences in the turbulent fluid behaviour, but none of the inlet has been better for internal flow in diesel injectors:

- by using a constant pressure inlet, velocity and oscillations similar to the experimentally obtained are calculated, but the required time is high and the inlet does not have the structure of the turbulence;
- by using a turbulent inlet condition, the required time decreases significantly, though the calculus is more unstable and the fluctuations do not have the coherent structure of the turbulence neither;
- and by using the mapped inlet condition the calculus is stable and less simulated time is required to get stabilized flow, but no turbulence is generated in a reasonable time.

However, considering the presented results the next solution to improve the simulation is purposed:

1. using the constant pressure inlet until the exit velocity reaches values close to the real ones,
2. then change the inlet condition to turbulent inlet to generate oscillations faster,
3. and finally switch to a direct mapped to stabilize the flow, obtain real turbulent structures and simulate more time.

This combination will be case dependent.

Acknowledgments

This work has been funded by *UNIVERSIDAD POLITÉCNICA DE VALENCIA* from Spain, in the framwork of the project "ESTUDIO DE LA INFLUENCIA DEL LEVANTAMIENTO DE AGUJA EN EL PROCESO DE INYECCION DIESEL", Reference No. PAID-06-10-2362.

The authors would like to thank *Universidad de Valencia* for the computer resources, technical expertise, the assistance provided and for allowing the use of supercomputer *Tirant*.

References

References

[1] N. Jarrin, S. Benhamadouche, D. Laurence, R. Prosser, A synthetic-eddy-method for generatirng inflow conditions for large-eddy simulations, International Journal of Heat and Fluid Flow 27 (2006) 585–593.

[2] C. Fureby, G. Tabor, H. G. Weller, A. D. Gosman, A comparative study of subgrid scale models in homogeneus isotropic turbulence, Physics of Fluids 9 (1997) 1416–1429.

[3] R. Payri, B. Tormos, J. Gimeno, G. Bracho, The potential of large-eddy simulation (les) code for the modeling of flow in diesel injectors, Mathematical and Computer Modelling 52 (2010) 1151–1160.

[4] G. R. Tabor, M. H. Baba-Ahmadi, Inlet conditions for large eddy simulation: a review, Computer & Fluids 39 (2009) 553–567.

[5] R. Payri, F. J. Salvador, J. Gimeno, J. de la Morena, Influence of injector technology on injection and combustion development - part 1: Hydraulic characterization, Applied Energy 88 (2011) 1064–1074.

[6] J. Benajes, R. Payri, S. Molina, A. H. Plazas, Investigation of the influence of injection rate shaping on the spray characteristics in a diesel common rail system equipped with a piston amplifier, Journal of Fluids Engineering-Transactions of the ASME 127 (2005) 1102–1110.

[7] R. Payri, F. J. Salvador, J. Gimeno, J. de la Morena, Study of cavitation phenomena based on a technique for visualizing bubbles in a liquid pressurized chamber, International Journal of Heat and Fluid Flow 30 (2009) 768–777.

[8] R. Payri, B. Tormos, J. Gimeno, G. Bracho, Large eddy simulation for high pressure flows: model extension for compressible liquids, Mathematical and Computer Modelling 54 (2011) 1725–1731.

[9] R. Payri, F. J. Salvador, J. Gimeno, A. García, Flow regime effects over non-cavitating diesel injection nozzles, Proceedings of the Institution of Mechanical Engineers, Part D, Journal of Automobile Engineering In Press, Corrected Proof (2011) –. doi:10.1177/0954407011413056.

[10] R. Payri, F. J. Salvador, J. Gimeno, G. Bracho, The effect of temperature and pressure on thermodynamic properties of diesel and biodiesel fuels, Fuel 90 (2011) 1172–1180.

[11] E. de Villiers, The potential of large eddy simulation for the modeling of wall bounded flows, Ph.D. thesis, Department of Mechanical Engineering, Imperial College of Science, Technology and Medicine (2006).

[12] O. Ltd., Foam - the complete guide, `http://www.opencfd.co.uk` (2011).

[13] F. J. Salvador, J. V. Romero, M. D. Roselló, J. Martínez-López, Validation of a code for modeling cavitation phenomena in diesel injector nozzles, Mathematical and Computer Modelling 52 (2010) 1123–1132.

[14] U. Piomelli, Large-eddy simulation: achievements and challenges, Progress in Aerospace Sciences (1999) 335–362.
[15] P. Sagaut, Large Eddy Simulation for Incompressible Flows, Springer, Berlin, 2001.
[16] R. Payri, J. M. García, F. J. Salvador, J. Gimeno, Using spray momentum flux measurements to understand the influence of diesel nozzle geometry on spray characteristics, Fuel 84 (2005) 551–561.